Applied Bionics and Biomechanics
Vol. 6, No. 1, March 2009, 73–85

Taylor & Francis
Taylor & Francis Group

Self-stabilising quadrupedal running by mechanical design

Panagiotis Chatzakos and Evangelos Papadopoulos*

Department of Mechanical Engineering, National Technical University of Athens, Athens, Greece

(*Received 8 August 2008; final version received 4 March 2009*)

Dynamic stability allows running animals to maintain preferred speed during locomotion over rough terrain. It appears that rapid disturbance rejection is an emergent property of the mechanical system. In running robots, simple motor control seems to be effective in the negotiation of rough terrain when used in concert with a mechanical system that stabilises passively. Spring-like legs are a means for providing self-stabilising characteristics against external perturbations. In this paper, we show that a quadruped robot could be able to perform self-stable running behaviour in significantly broader ranges of forward speed and pitch rate with a suitable mechanical design, which is not limited to choosing legs spring stiffness only. The results presented here are derived by studying the stability of the passive dynamics of a quadruped robot running in the sagittal plane in a dimensionless context and might explain the success of simple, open loop running controllers on existing experimental quadruped robots. These can be summarised in (a) the self-stabilised behaviour of a quadruped robot for a particular gait is greatly related to the magnitude of its dimensionless body inertia, (b) the values of hip separation, normalised to rest leg length, and leg relative stiffness of a quadruped robot affect the stability of its motion and should be in inverse proportion to its dimensionless body inertia, and (c) the self-stable regime of quadruped running robots is enlarged at relatively high forward speeds. We anticipate the proposed guidelines to assist in the design of new, and modifications of existing, quadruped robots. As an example, specific design changes for the Scout II quadruped robot that might improve its performance are proposed.

Keywords: quadruped robot; dynamic running; dynamic similarity; passive dynamics; self-stability; mechanical design

1. Introduction

Negotiation of rough terrain is the most important reason for building legged robots, instead of wheeled and tracked ones. Animals exhibit impressive performance in handling rough terrain and they can reach a much larger fraction of the earth landmass on foot than existing wheeled vehicles. Their robotic counterparts have not yet been benefited from the improved mobility and versatility that legs offer. Early attempts to design legged platforms resulted in slow moving, statically stable robots, which are still the most prevalent today (see Berns 2008 for a survey).

In this paper, however, we focus on dynamically stable legged robots. Two decades ago, Raibert (1986) set the stage with his groundbreaking work on dynamic legged locomotion by introducing very simple controllers for stabilising running on his one-, two- and four-legged robots. Later on, Buehler (2002) designed and built power autonomous legged robots with one, four and six legs, which demonstrate walking and running in a dynamic fashion. The underlying fundamental principles exemplified by his robots were minimal actuation, coupled with a suitably designed mechanical system featuring springy legs, and simple control laws that excite the natural dynamics of the mechanical system.

Patrush and Tekken robotic quadrupeds by Kimura et al. (2007) are examples of another design and control approach for dynamically stable running. On the basis of principles from neurobiology, Kimura et al. proposed a controller based on a Central Pattern Generator (CPG) that alters its active phase based on sensory feedback and results in adaptive dynamic walking on irregular terrain.

Despite their morphological and design differences all these robots are propelled forward using control laws without intense feedback. For instance, Poulakakis et al. (2006) demonstrated recently on the quadrupedal robot Scout II that simple controllers, requiring only touchdown detection and local feedback from motor encoders, can be used to stabilise running. These controllers simply position the legs at a fixed touchdown angle during the flight phase and result in stable bounding.

In a non-literal sense, these experimental findings in robotics are in qualitative agreement with developments in biology. As experimental evidence suggests, the high-level nervous system is not required for steady-state level walking and running, and mechanisms entirely located within the spinal cord are responsible for generating the rhythmic motions of the legs during locomotion (see McMahon 1985 and Pearson 1976).

*Corresponding author. Email: egpapado@central.ntua.gr

ISSN: 1176-2322 print / 1754-2103 online

DOI: 10.1080/11762320902863908
http://www.informaworld.com

Furthermore, control during rapid locomotion is dominated by the mechanical system as recent research in physiology indicates (see Kubow and Full 1999 and Full and Koditschek 1999). Kubow and Full developed a simple, two-dimensional, dynamic model of a hexapedal runner to explore the role of the mechanical system in control. This model had no equivalent of nervous feedback and it was surprisingly found to be inherently stable. This pioneering work first revealed the significance of the mechanical system in simplifying control by demonstrating that stability could result from leg moment arm changes alone. Therefore, it is reasonable to assume that intense control action relying on complex feedback from multiple sensors is not necessary to generate and sustain walking and running.

In an attempt to study the basic properties of sagittal plane running, Schwind (1998) proposed the Spring Loaded Inverted Pendulum (SLIP) template, which, despite its structural simplicity, was found to sufficiently encode the task-level behaviour of animals and robots. These early results were also confirmed by Full and Koditschek (1999), who further set the basis for a systematic approach in studying legged locomotion by introducing the templates and anchors modelling and control hierarchy.

In addition, recent research conducted independently by Seyfarth et al. (2002) and Ghigliazza et al. (2003) showed that when the SLIP is supplied with the appropriate initial conditions and for certain touchdown angles, not only does it follow a cyclic motion, but it also tolerates small perturbations without the need of a feedback control law. This inherent stability of the SLIP model is a very interesting property.

The formal connection between templates, such as the SLIP, and more elaborate models, which enjoy a more faithful correspondence to the morphology of the robot, has not yet been fully investigated (for preliminary results, see Saranli and Koditschek 2003). Also, as was shown by Cherouvim and Papadopoulos (2005), controllers specifically derived for the SLIP will have to be modified in order to be successful in inducing stable running in more complete models that include pitch dynamics and comprise energy losses.

However, simplified models have been proved to be helpful in the design of controllers that exploit the passive dynamics of the system, resulting in considerable energy savings, which is a critical requirement for autonomous legged locomotion. A notable example of such controllers is the one in ARL's Monopod II at McGill by Ahmadi and Buehler (1997) and the one by Papadopoulos and Cherouvim (2004). It is also generally accepted that running is essentially a natural mode of the system and that only minor control and energy effort are required to maintain motion.

In this paper, motivated by the experimental findings in existing robots, we attempt to provide an explanation for simple control laws being adequate in stabilising complex running tasks, such as bounding. It is the simplicity of these robots' design and control, together with experimental success, that initiated our attempts for this work. Our analysis departs from the recent developments regarding the self-stabilisation property of quadruped robots, such as Scout II by Poulakakis et al. (2006), where it is shown that the dynamics of the open loop passive system alone can confer stability of motion. It was found that bounding gaits can be passively generated as a response of the system to an appropriate set of initial conditions and a regime where the system is self-stabilised against small perturbations from the nominal conditions was identified. However, this regime involved running with forward speeds of 3–4 $m \cdot s^{-1}$ and bounding with 100–200 $deg \cdot s^{-1}$ (pitch rate), which is not practically achievable with existing quadruped robots.

In our work, the stability analysis of the passive dynamics of robotic quadrupeds is studied in a dimensionless context (Chatzakos and Papadopoulos 2009), revealing further intrinsic properties of quadrupedal running and unveiling aspects of robotic quadrupeds that have a similar configuration but a different scale. It is shown that a suitable quadruped mechanical design can provide self-stabilising characteristics against external perturbations that originate in leg–ground interactions or in motor control. This results in dynamically stable running with bounding gaits with physically realistic and practically achievable forward speeds and pitch rates. We anticipate the guidelines proposed hereinafter to assist in the design of new, and modifications of existing, quadruped robots.

To investigate passive stability, a simple mechanical model of a quadruped robot running in the sagittal plane that encodes the targeted task-level behaviour (steady-state bounding) is employed. The model is unactuated and conservative, so that the properties of the natural dynamics of the system can be revealed. It includes pitching, which is a very important component of the motion that is not captured by point-mass models like the SLIP. To broaden our analysis and reveal the effect of scaling, dimensional analysis is employed to this model. It will be shown that the proposed conservative model of the quadruped robot can passively bound for a wide range of robot physical parameters and rapidly reject disturbances, as an emergent property of suitable mechanical system design, to maintain running.

To identify conditions that permit the generation of passive running cycles and study their stability properties, a Poincaré return map, whose fixed points describe the cyclic bounding motion, is derived and studied numerically. Bounding and pronking (essentially bounding with no body pitching) gaits, which are of great experimental interest in existing quadruped robots, are analysed. It is found that both can be passively generated as a response of the system to an appropriate set of initial conditions. Parametric regions, where the system is self-stabilised against small perturbations from the nominal conditions, are identified.

Hence, proper selection of new robots', or modification of existing robots', physical parameters might result in enlarged regions of stable running, i.e. perform self-stable running behaviour in significantly broader ranges of running speed and control parameters.

It is worth mentioning that the early results from similar approaches adopted to study quadrupedal running in the past (see Iida and Pfeifer 2004, Zhang et al. 2004 and Poulakakis et al. 2006) are confirmed by our study. We therefore believe that the proposed guidelines, which are described in detail in Section 3, are plausible in the real world and might be used to extend the self-stable behaviour of quadruped running robots through inspired mechanical design. Furthermore, our results might also explain the success of simple, open loop running controllers on existing experimental quadruped robots and facilitate the design of legged locomotion controllers that take advantage of the system's natural dynamics.

2. Methods

In this section we introduce a simple model, i.e. a template, for studying and analysing gaits where the pitching motion is a significant mode in the system's motion, e.g. bounding or pronking. Inspired by the SLIP model (Schwind 1998), which exhibits natural stability, we aim at identifying a template for studying the dynamics of gaits with body pitching motion. Note that the stability of bounding and pronking gaits cannot be studied using the SLIP as a template, since this model does not capture the body's oscillatory pitching motion.

As soon as the appropriate template of the physical model is defined, which is a set of dependent and independent variables and all of the parameters that are thought to be significant, the complete equations made from this list of variables will be manipulated to be independent of the choice of units, i.e. dimensionless. The non-dimensional variables will then be formed into groups that define the morphology of the quadruped robot or that correspond to ratios of robot physical parameters in the model equations, such as the Reynolds number or Froude number (Alexander 1977; Reynolds 1883) that often arise in models of geophysical fluid dynamics.

The resulting model will be used next to analyse the passive dynamic behaviour, i.e. the unforced response, of the system. Understanding the properties of a passive and conservative model is crucial for deriving mechanical design (and controllers), which will exploit its passive dynamics. The control action should aim to help the robot move in the way it wishes to move, while the mechanical design should excite its natural dynamics. As a result, the effort of the actuators can be reduced, leading to increased power efficiency. Moreover, the complexity of the system design is significantly reduced, thus increasing the reliability and decreasing the cost. The core of this approach is to find mechanical design principles to excite the dynamics of the system and enlarge the domain of attraction of the passively generated cyclic motion. This will be greatly facilitated by identifying the main parameters that affect the motion of the system and by finding conditions among the variables that lead to passive cyclic motion.

Since dynamically stable running gaits are to be studied, techniques drawn from modern dynamical systems theory will be used. To this end, a return map that describes the bounding motion will be numerically constructed. Then a searching procedure for finding its fixed points will be proposed. In doing so, the Newton–Raphson method will be employed. A large number of fixed points are generated by this method. All of these fixed points possess symmetric properties, which are very useful in making the search procedure systematic. This will be apparent in the next section, where most of the analysis is undertaken.

2.1. Template

The complexity of four-legged animals and robots can be reduced to relatively simple models, that can then be used to analyse a system's behaviour, by taking into account synergies, i.e. parts that work together in coordinated action or operation, and symmetries, i.e. the correspondence of parts on opposite sides of a plane through body (Full and Koditschek 1999). By synergies, we mean parts that work together in combined action or operation, e.g. groups of muscles, joints, legs, etc. By symmetries we mean the correspondence of parts on opposite sides of a plane through the body.

In this section we use a simple model, i.e. a template, for studying and analysing gaits where the pitching motion is a significant mode in the system's motion, e.g. the bound and the pronk. Pronking is essentially bounding with no body pitching, and has only the flight and double stance phases. Although pronking may reduce in practice to bounding with very limited pitching, it does offer advantages in control design. Note that bounding and pronking gaits cannot be studied using the SLIP as a template, since this model does not capture the body's oscillatory pitching motion.[1] To this end, such a template, which is commonly used to analyse the basic qualitative properties of quadrupedal running in the sagittal plane, is shown in Figure 1, while its associated parameters needed to describe it are given in Table 1.

As shown in Figure 1, the planar model represents the lateral half of a quadruped, and consists of a rigid body

[1] A pronking animal or robot does not pitch at all, only a bounding one does. Consequently, the SLIP can be used to study the pronk. However, in real situations the robot is continuously perturbed and the SLIP does not capture such disturbances in body's pitching motion. Therefore, it cannot be used to study a system's stability properties and examine whether these disturbances decay in subsequent steps resulting to stable pronk or they grow and eventually repetitive motion is lost.

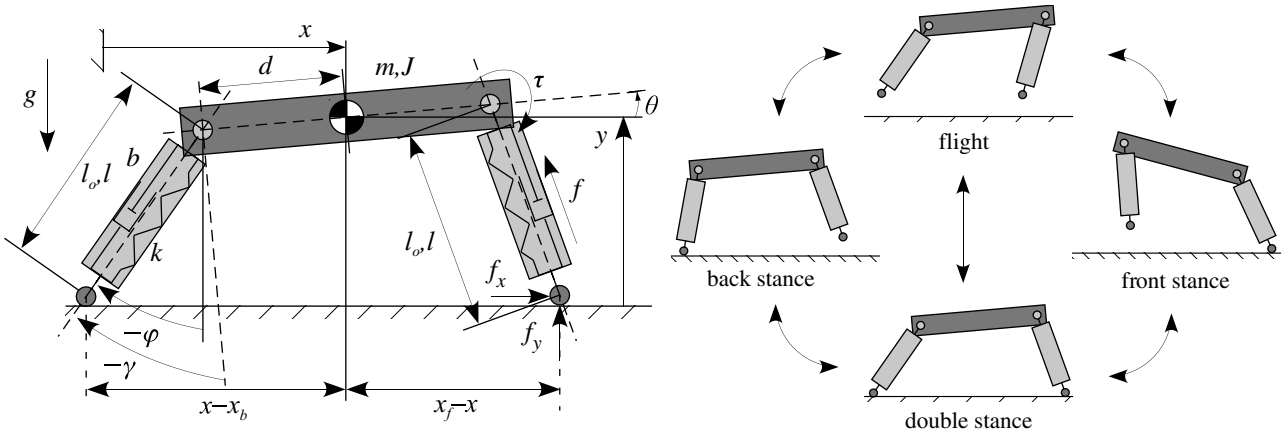

Figure 1. Parameters of the template for quadrupedal running in plane and gait phases.

and two springy massless legs, attached to either side of the body. Actuators control the angle of each leg with respect to the body and the torque delivered by each leg. Each modelled leg represents the back or the front leg pair, in which the two back or front legs are always in phase and is called the virtual leg (Raibert 1986). Each virtual leg has twice the stiffness of the robot leg and includes friction modelling, as the sum of Coulomb and viscous friction. The torque delivered at each hip and the force along each robot leg is equal to half the corresponding ones at the virtual leg.

The gaits referred to are the pronk, in which all the robot legs are always in phase, and the bound, in which the back pair of legs is in phase, as is the front pair. The bound may involve up to four motion phases, while the pronk has only the double stance and flight phases. Note that this model can also be used to study other sagittal plane running gaits, such as pacing, or trotting, in which the stability of pitching motion is important and cannot be modelled by point-mass hoppers like the SLIP.

System dynamics are derived using a Lagrangian formulation, with generalised coordinates to be the Cartesian variables describing the centre of mass (COM) position and the main body's attitude. During flight, the robot is under the influence of gravity only. Throughout the stance phase, the robot's toes are fixed on the ground and act as lossless pivot joints. The dynamics for any phase may be derived from that of the double stance by removing appropriate terms. Hence, only the double stance dynamics is given in the form of a set of differential and algebraic equations:

$$\begin{aligned} m\ddot{x} = &-(f_b + k\,(l_o - l_b) - f_{fr,b})\sin\gamma_b - \tau_b\cos\gamma_b/l_b \\ &-(f_f + k(l_o - l_f) - f_{fr,f})\sin\gamma_f - \tau_f\cos\gamma_f/l_f \end{aligned} \tag{1}$$

Table 1. Variables and indices used.

Symbol	Units	Variable	Symbol	Units	Variable
x	m	COM horizontal pos.	b	Nt·m·s^{-1}	Damping coefficient
y	m	COM vertical pos.	h_{apex}	m	Flight apex position
θ	deg	Body pitch angle	g	M·s^{-2}	Acceleration of gravity
γ	deg	Leg absolute angle	m	kg	Body mass
φ	deg	Leg relative angle	J	kg·m^{-2}	Body inertia
x_{bt}	m	Back toe horizontal pos.	d	m	Hip joint to COM distance
x_{ft}	m	Front toe horizontal pos.	f	—	As index: front leg
l	m	Leg length	b	—	As index: back leg
l_o	m	Leg rest length	j	—	Dimensionless body inertia
k	Nt·m^{-1}	Leg spring stiffness	r	—	Relative leg stiffness
τ	Nt·m	Torque delivered at hip	p	—	Dimensionless hip separation
f	Nt	Axial force at leg	Fr	—	Froude number
f_{fr}	Nt	Overall friction force	s	—	Time scale
f_c	Nt	Coulomb friction	$*$	—	As superscript: dimensionless

$$m\ddot{y} = (f_b + k(l_o - l_b) - f_{fr,b})\cos\gamma_b - \tau_b \sin\gamma_b/l_b + (f_f + k(l_o - l_f) - f_{fr,f})\cos\gamma_f - \tau_f \sin\gamma_f/l_f - mg \quad (2)$$

$$J\ddot{\theta} = \tau_b - d(f_b + k(l_o - l_b) - f_{fr,b})\cos(\gamma_b - \theta) + \tau_f + d(f_f + k(l_o - l_f) - f_{fr,f})\cos(\gamma_f - \theta) + d\tau_b \sin(\gamma_b - \theta)/l_b - d\tau_f \sin(\gamma_f - \theta)/l_f \quad (3)$$

where

$$\gamma_b = \operatorname{atan2}(y - d\sin\theta, x_{bt} + d\cos\theta - x)$$
$$\gamma_f = \operatorname{atan2}(y + d\sin\theta, x_{ft} - d\cos\theta - x) \quad (4)$$
$$l_b = \sqrt{(x_{bt} - x + d\cos\theta)^2 + (d\sin\theta - y)^2}$$
$$l_f = \sqrt{(x_{ft} - x - d\cos\theta)^2 + (d\sin\theta + y)^2} \quad (5)$$
$$f_{fr,i} = f_c \operatorname{sign}(\dot{l}_i) + b\dot{l}_i, \quad i = b, f. \quad (6)$$

2.2. Scaling

Dimensional analysis can be applied to all quantitative models and offers an efficient way to display complex datasets. Usually, it makes the subsequent analysis much more useful, because the physical model, as first written, is rather general. The premise of dimensional analysis is that complete equations can be written in a form that is independent of the choice of units, and variables appear in combinations that are dimensionless. For our study, such dimensionless variables are introduced as follows:

$$t^* = \frac{t}{s} \quad (7)$$

$$x^* = \frac{x}{l_o}, \quad \dot{x}^* = s\frac{\dot{x}}{l_o}, \quad \ddot{x}^* = s^2\frac{\ddot{x}}{l_o} \quad (8)$$

$$y^* = \frac{y}{l_o}, \quad \dot{y}^* = s\frac{\dot{y}}{l_o}, \quad \ddot{y}^* = s^2\frac{\ddot{y}}{l_o} \quad (9)$$

$$\theta^* = \theta, \quad \dot{\theta}^* = s\dot{\theta}, \quad \ddot{\theta}^* = s^2\ddot{\theta} \quad (10)$$

where s is the time scale of the system, and the rest of the variables are defined in Table 1.

By substituting (7)–(10) into the equations of motion, given by (1)–(6), one gets a dimensionless description of the system. The resulting motion of the COM is then characterised by a time scale, which is associated to the inverse of the natural frequency of the horizontal motion:

$$\frac{s^2 g}{l_o} = 1 \Rightarrow s = \sqrt{\frac{l_o}{g}}. \quad (11)$$

Selection of this particular time scale of the system results in a number of dimensionless parameter groups, which are widely used by experimental biologists. These include: (a) the Froude number *Fr* (Alexander 1977), defined as

$$Fr = \frac{v}{\sqrt{g l_o}} \quad (12)$$

where v is the robot forward speed, (b) the dimensionless body inertia j (Murphy and Raibert 1984), i.e. the robot's body inertia normalised to md^2:

$$j = \frac{J}{md^2} \quad (13)$$

and (c) the leg relative stiffness r (Blickhan 1989), which is given as

$$r = \frac{kl_o}{mg}. \quad (14)$$

Since we are primarily interested in the forward motion aspects, the choice of the time scale, as in (11), is advantageous and will be used next to set the equations of motion dimensionless. While the individual dimensionless equations would be different if one uses a different time scale, the relationships between them would be invariant.

The following dimensionless parameters are also introduced: (a) the normalised half hip separation p:

$$p = \frac{d}{l_o} \quad (15)$$

and (b) the dimensionless viscous friction coefficient b^*:

$$b^* = \frac{b}{m}\sqrt{\frac{l_o}{g}} \quad \text{or} \quad b^* = 2\zeta\sqrt{r} \quad (16)$$

where ζ is the damping ratio.

Force and torque variables are finally normalised as

$$f_i^* = \frac{f_i}{mg}, \quad i = b, f, c \quad \text{and} \quad \tau_i^* = \frac{\tau_i}{mg\, l_o}, \quad i = b, f. \quad (17)$$

The desired dimensionless description of the system results from substituting (7)–(11) and (13)—(17) to (1)–(6), and it is presented next for the double stance:

$$\ddot{x}^* = (f_{fr,b}^* - f_b^* - r(1 - l_b^*))\sin\gamma_b^* - \tau_b^*/l_b^* \cos\gamma_b^* + (f_{fr,f}^* - f_f^* - r(1 - l_f^*))\sin\gamma_f^* - \tau_f^*/l_f^* \cos\gamma_f^* \quad (18)$$

$$\ddot{y}^* = (f_b^* + r(1 - l_b^*) - f_{fr,b}^*)\cos\gamma_b^* - \tau_b^*/l_b^* \sin\gamma_b^* + (f_f^* + r(1 - l_f^*) - f_{fr,f}^*)\cos\gamma_f^* - \tau_f^*/l_f^* \sin\gamma_f^* - 1 \quad (19)$$

$$pj\ddot{\theta}^* = -(f_b^* + r(1 - l_b^*) - f_{fr,b}^*)\cos(\gamma_b^* - \theta^*) + (f_f^* + r(1 - l_f^*) - f_{fr,f}^*)\cos(\gamma_f^* - \theta^*) + \tau_b^*/p + \tau_f^*/p + \tau_b^* \sin(\gamma_b^* - \theta^*)/l_b^* - \tau_f^* \sin(\gamma_f^* - \theta^*)/l_f^* \quad (20)$$

where

$$\gamma_b^* = \mathrm{atan2}(y^* - p\sin\theta^*, x_{bt}^* + p\cos\theta^* - x^*)$$
$$\gamma_f^* = \mathrm{atan2}(y^* + p\sin\theta^*, x_{ft}^* - p\cos\theta^* - x^*) \quad (21)$$

$$l_b^* = \sqrt{(x_{bt}^* - x^* + p\cos\theta^*)^2 + (p\sin\theta^* - y^*)^2}$$
$$l_f^* = \sqrt{(x_{ft}^* - x^* - p\cos\theta^*)^2 + (p\sin\theta^* + y^*)^2} \quad (22)$$

$$f_{fr,i}^* = f_c^* sign(\dot{l}_i^*) + b^* \dot{l}_i^*, \quad i = b, f. \quad (23)$$

2.3. Similarity

A similarity rule maintains the constancy of a non-dimensional number. The simplest similarity rule is geometric similarity. Here, the ratio of any lineal dimension to a characteristic length of the system is constant and all dimensions are magnified by the same factor as compared to a base configuration. For example, if the same materials are used, the mass of a system scales with the cube of the length in geometrically similar systems.

Just as geometric similarity refers to shapes, the concept of dynamic similarity refers to motion. Two motions are said to be dynamically similar if one could be made identical to the other by multiplying all linear dimensions by some constant factor and all time intervals by another. Additionally, dynamic similarity in legged locomotion requires that the Froude numbers of the motions of two quadruped animals (or robots) are equal (Alexander 1977).

According to the dimensional analysis presented previously and by observing the dimensionless description of the system, given by (18)–(23), dynamically similar motions require further that the dimensionless parameters in (13)–(15) are equal for motions with the same characteristics, e.g. flight apex, body pitch angle and pitch rate. Repeating for clarity, these parameters, which are connected to robot morphological characteristics, are: (a) the dimensionless body inertia j, (b) the leg relative stiffness r and (c) the normalised half hip separation p, defined in (13), (14) and (15), respectively.

Next, we use an evidential example based on biological data to show similarity requirements. Let the rest leg length be the characteristic scale length. This implies that by doubling the rest length of the leg, the robot is scaled up by a factor of two. Body mass is proportional to the third power of the characteristic length, while the gravitational acceleration does not scale with size. Therefore, in order for the robot to keep moving in a dynamically similar fashion, the leg stiffness should be quadruplicated, see (14), since the relative stiffness of the leg should be kept constant. This is consistent with biology findings in animal scaling laws by Farley et al. (1993), where the leg springiness increases with body mass, i.e. $k \propto m^{2/3}$.

2.4. Analysis

It is generally accepted that bounding is essentially a natural mode of the system, and that only minor control and energy effort are required to maintain running. Practically, this motivated us to study the passive dynamics of the system. With the term passive dynamics, we mean the unforced response of the system under a set of initial conditions. The goals of the analysis are to determine the conditions required to permit steady-state cyclic motion, to understand the fundamentals of the bounding gait followed by the robot and to find ways to apply these results to improve the performance of quadruped robots.

The practical motivation for studying passive bounding is power efficiency. Indeed, if the cyclic motion is generated passively, then the actuators have less work to do to maintain the motion, since they do not 'push' the robot towards motions that are against its natural dynamics. Furthermore, if there are operating regimes where the system is passively stable, then active stabilisation is not required and the motors of the robot will only compensate for energy losses. For instance, using passive running, Ahmadi and Buehler (1997) reported energy savings of 93%. On the other hand, maintaining the preferred speed during locomotion over rough terrain appears to require rapid disturbance rejection, which should be an intrinsic property of the mechanical system, especially at high speeds, and studying passive bounding will reveal the characteristics that can provide self-stabilising behaviour.

Overall, the benefits of an approach based on the passive dynamics of the system are multiple, especially in simplifying the mechanical electrical and electronic design and in extending the operational range of the robot. The unactuated and conservative model that will be used in our analysis is derived from (18) to (23) by eliminating actuation and energy dissipation terms. It is given here for completeness:

$$\ddot{x}^* = -r(1 - l_b^*)\sin\gamma_b^* - r(1 - l_f^*)\sin\gamma_f^* \quad (24)$$

$$\ddot{y}^* = r(1 - l_b^*)\cos\gamma_b^* + r(1 - l_f^*)\cos\gamma_f^* - 1 \quad (25)$$

$$\ddot{\theta} = r((1 - l_f^*)\cos\phi_f^* - (1 - l_b^*)\cos\phi_b^*)/pj \quad (26)$$

$$\gamma_b^* = \operatorname{atan2}(y^* - p\sin\theta^*, x_{bt}^* + p\cos\theta^* - x^*)$$

$$\gamma_f^* = \operatorname{atan2}(y^* + p\sin\theta^*, x_{ft}^* - p\cos\theta^* - x^*) \quad (27)$$

$$l_b^* = \sqrt{(x_{bt}^* - x^* + p\cos\theta^*)^2 + (p\sin\theta^* - y^*)^2}$$

$$l_f^* = \sqrt{(x_{ft}^* - x^* - p\cos\theta^*)^2 + (p\sin\theta^* + y^*)^2} \quad (28)$$

$$f_{fr,i}^* = f_c^*\,\mathrm{sign}(\dot{l}_i^*) + b^*\dot{l}_i^*, \quad i = b, f. \quad (29)$$

In order to evaluate the performance of the above model, we focus on system periodic steady-state trajectories, which are identical trajectories that repeat themselves during locomotion. Following a procedure similar to Zhang et al. (2004) and Poulakakis et al. (2006), we employ a Poincaré Map technique to formulate these trajectories. The return map connects the system state at a well-defined locomotion event to the state of the same event at the next cycle. Here, this event is chosen to be the apex height. We could select any other point in the cycle. However, the selection of the apex height allows for the touchdown angles of both the front and back virtual legs to explicitly appear in the definition of the return map as kinematic inputs available for control. Note also that the vertical velocity at apex height is always zero, which reduces the dimensions of the state vector. A second dimensional reduction to the state vector can be obtained by projecting out the horizontal component x of the state vector, since it is not relevant to describing the running gait, i.e. the distance travelled has no influence on the locomotion cycle. This also resolves the issue that the horizontal component x does not map to itself after a cycle, since it will never be identical between two successive apex height points. This is because the forward distance travelled during one stride is always non-zero for non-zero forward speeds. Thus, the state vector $\mathbf{x}^*$ at apex height consists of the apex height, the body pitch angle, the forward speed and the body pitch rate only, i.e.

$$\mathbf{x}^* = \left[\, y^* \;\; \theta^* \;\; \dot{x}^* \;\; \dot{\theta}^* \,\right]. \quad (30)$$

The state vector at apex height for some cycle n, $\mathbf{x}_n^*$, constitutes the initial conditions. On the basis of these, the flight equations, derived from (24) to (29) by removing terms not permanent to the phase, are integrated until one of the touchdown events occurs, e.g. front or back leg stance (see Figure 1). The touchdown event triggers the next phase, whose dynamics are integrated using the final conditions of the previous state as initial conditions. Depending on system configuration, the next phase could be either flight, i.e. bounding without double stance, or double stance. Pronking is the case of bounding with zero body pitch rate and the touchdown event following flight is the double stance, which is in turn followed by flight, i.e. there is no back or front leg stance phase.

Successive forward integration of the dynamic equations of all the phases yields the state vector at apex height of the next stride, which is the value of the Poincaré return map $\mathbf{F}$. If the state vector at the new apex height is identical to the initial one, the cycle is repetitive and yields a fixed point. Mathematically, this is given as

$$\mathbf{x}_{n+1}^* = \mathbf{F}(\mathbf{x}_n^*, u_n^*) \quad (31)$$

where $u^* = [\,\gamma_{b,td}^* \;\; \gamma_{f,td}^*]$ includes the inputs, which are the touchdown angles, back and front leg. Despite the fact that the touchdown angles are not part of the state vector and these do not participate in the dynamics, they directly affect the value of the return map. It is apparent from (31) that the touchdown angles are kinematic inputs available for 'cheap' control, since it is very easy to place the legs at their target angles during the flight phase in most of the quadruped robots.

It is important to note here that in calculating the return map any possible sequence of the phases, which result in different phases, e.g. symmetric bounding motion where flight occurs after back leg stance double instead of double stance or pronking, was considered. It must also be noted that existence of such fixed points seems to be the rule, rather than the exception.

In order to determine the conditions required to result in steady-state cyclic motions, we resort to a numerical evaluation of the return map using a Newton–Raphson method. By employing this method, a large number of fixed points can be found for different initial conditions and different touchdown angles. These angles, although not part of the state vector and not generalised coordinates, directly affect the value of the return map as they determine touchdown and liftoff events and impose constraints on the motion of robot during back/front leg and double stance phases. Variant dimensionless combinations of robot's physical parameters, as defined in (13)–(15), also result in different fixed points. These design parameters vary between their extreme values found either in experimental biology references, Farley et al. (1993) and Herr et al. (2002), or are imposed by common sense. Particularly, they range as follows:

$$j = 0.70 - 1.45, \quad r = 10 - 30, \quad p = 0.25 - 1.00. \quad (32)$$

2.5. Stability

The existence of passively generated bounding running cycles is by itself a very important result, since it shows that an activity so complex as bounding running can simply be a natural motion of the system. However, in real situations the robot is continuously perturbed, therefore, if the fixed point were unstable, then the periodic motion would not be sustainable. It would therefore be important to study the stability properties of the fixed points found above and to design controllers to improve the robustness of the system against perturbations. In this section, we characterise the stability of the fixed points using local stability analysis, i.e. using the eigenvalues of the linearised return map.

The stability analysis is based on linearising the non-linear map about a fixed point. A set of linearised equations specifies how a perturbation on the steady cycle propagates from one cycle to the next. The problem of stability in discrete-time systems, such as the return map derived in the previous section, is different from the continuous-time case, because of the different stability domain in the complex plane. The left half of the complex plane in the continuous time systems is replaced by the inside of the unit circle. Calculating the system's eigenvalues and checking whether or not they are inside the unit circle can verify stability for discrete-time systems. Therefore, to investigate stability, we assume that the apex height states are perturbed from their steady-cycle values $\bar{\mathbf{x}}$, by some small amount $\Delta\mathbf{x}$. The model that relates the deviations from steady state, i.e. the incremental or small-signal model, is

$$\Delta\mathbf{x}^*_{n+1} = \left.\frac{\partial\mathbf{F}(\mathbf{x}^*, \mathbf{u}^*)}{\partial\mathbf{x}}\right|_{\mathbf{x}=\bar{\mathbf{x}}} \Delta\mathbf{x}^*_n + \left.\frac{\partial\mathbf{F}(\mathbf{x}^*, \mathbf{u}^*)}{\partial\mathbf{u}}\right|_{\mathbf{u}=\bar{\mathbf{u}}} \Delta\mathbf{u}^*_n \tag{33}$$

with $\Delta\mathbf{x}^* = \mathbf{x}^* - \bar{\mathbf{x}}^*$ and $\Delta\mathbf{u}^* = \mathbf{u}^* - \bar{\mathbf{u}}^*$. For small perturbations, the apex height states at the next stride can be calculated by (33), which is a linear difference equation. If all the eigenvalues of the system matrix $\mathbf{A}$, where $\mathbf{A}$ is

$$\mathbf{A} = \left.\frac{\partial\mathbf{F}(\mathbf{x}^*, \mathbf{u}^*)}{\partial\mathbf{x}}\right|_{\mathbf{x}=\bar{\mathbf{x}}} \tag{34}$$

having magnitude less than one, then the periodic solution is stable and disturbances decay in subsequent steps. If not, then disturbances grow and eventually repetitive motion is lost.

3. Results

Using this systematic procedure for finding fixed points described previously, conclusions on how the system responds under a set of initial conditions can be drawn. Surprisingly, there are parametric regions where the system is stable without the need of a closed loop controller. The purpose of the analysis in this section is to quantify the properties of passively generated periodic motion for quadruped robots and to search for regions where the system can passively tolerate departures from the fixed points.

The major question is whether there exists a regime, where the system tolerates perturbations from the nominal conditions without requiring any closed loop control law. The existence of this regime raises an important 'philosophical' question: Is there a particular (and physically realistic) mechanical design that provides self-stabilising characteristics against external perturbations originated in leg–ground interactions or motor control? How much feedback is necessary then for developing control laws to stabilise a system, which exhibits inherent self-stability by means of suitable mechanical design? The answers to these questions are not yet available. However, the existence of such mechanical self-stabilised behaviours suggests that clock-based feed-forward control laws can excite the dynamics of the robot appropriately to exploit the inherent stability of the system. The added feedback can improve the robustness of those controllers. Therefore, we believe that results presented in this section constitute a beginning in the right direction.

To show how motion characteristics, such as forward speed and pitch rate, and mechanical design, i.e. combinations of robot physical parameters, affect the stability of the motion, we present figures (Figures 2–5) that display isolines of the magnitude of the larger eigenvalue of system matrix $\mathbf{A}$, as defined in (34). The largest eigenvalue norm is interpreted as heights with respect to the x–y plane, where x–y variables are either motion characteristics for the bounding gait, such as forward speed and pitch rate, or dimensionless combinations of robot physical parameters, as defined in (13)–(15), e.g. dimensionless body inertia, leg relative stiffness and normalised half hip separation. For certain values of these parameters the larger eigenvalue enters the unit circle, while the other eigenvalues remain well behaved. This fact shows that, for these parameter values, the system is self-stabilised. In all figures, the grey-hatched area corresponds to unstable regions, i.e. regions where at least one eigenvalue is located outside of the unit circle and the system is not passively stable. Broadly, we are looking for the size of the unstable region and how that changes. The magnitude of the 'non-participating' variables is shown in the title of each subplot in every figure.

3.1. Forward speed (Froude number)

Isolines of the largest eigenvalue norm at various pitch rates and values of dimensionless body inertia are displayed in Figure 2. The contour plots are drawn for dimensionless apex height 1.1, leg relative stiffness 12 and normalised half hip separation 0.85. The magnitude of these variables has been chosen such as to correspond to the physical parameters of Scout II (see Poulakakis et al. 2006). The reason for this choice is to demonstrate how an existing robot can

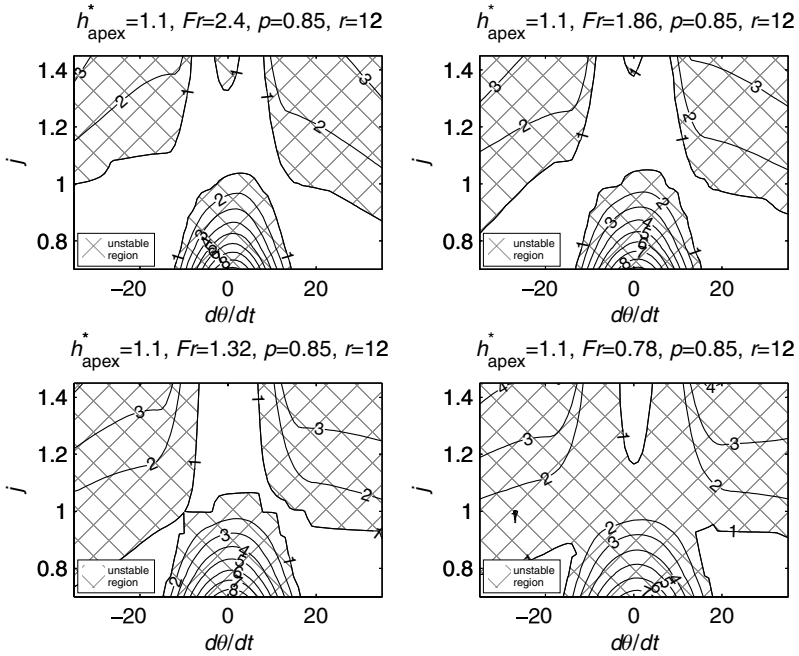

Figure 2. Largest eigenvalue norm at various pitch rates (x axis) and dimensionless body inertias (y axis) for dimensionless apex height 1.1, normalised half hip separations 0.85, leg relative stiffness 12 and forward speeds (Froude numbers) from 0.78 to 2.40 (subplots 1–4).

be mechanically modified in order to expand the domain of attraction of its self-stabilised behaviour.

The main conclusion from the analysis performed by Poulakakis et al. (2006) is that there exists a regime where the Scout II robot can be passively stable. This was an important result, since it showed that the system could tolerate small perturbations away from the nominal conditions without any control action taken. This fact could provide a possible explanation to why Scout II can bound without the need of complex state feedback, using very simple control laws that only excite its natural dynamics.

Similar findings are evident in Figure 2, where the four subplots have been plotted for dimensionless forward speeds (Froude number) from 2.40 to 0.78. For the particular mechanical design adopted for the Scout II robot, the self-stable regime, where all the eigenvalues lie inside the unit circle, is achieved for bounding at sufficiently high forward speeds. This was also reported in Poulakakis et al. (2006). However, as it can be deducted by Figure 2, by changing the value of dimensionless body inertia, the Scout II robot can expand its self-stable regime and passively bound at surprisingly lower forward speeds. It is simple for a robot to attain a specific value of dimensionless body inertia by proper hip placement or redistributing body mass.

Finding 1. Great forward speed favours the self-stabilised behaviour of quadruped robots, as it enlarges the regime where the mechanical system can reject rapid perturbations. When the quadruped robot is moving more slowly, the magnitude of dimensionless body inertia must take extreme values in order to sustain the self-stabilising characteristics: greater than one for low pitch rates and less than one for high pitch rates.

3.2. Dimensionless body inertia

According to Poulakakis et al. (2006), the largest eigenvalue obtained its maximum value when the pitch rate was small. Recall that the region where pitch rate takes small values corresponds to a pronking-like motion, where both the front and back legs hit and leave the ground in unison and pitch rate is minimised. Thus, they had concluded that pronking-like motions (low pitch rates) are 'more unstable' than bounding (high pitch rates). This fact was also observed in experiments with Scout II. As shown in Figure 2, this is true when the dimensionless body inertia is less than one. However, attaining a value of dimensionless body inertia that is greater than one could provide the Scout II robot with self-stabilising characteristics for pronking motions as well. Note that the lower the forward speed, the greater the value of dimensionless body inertia must be.

The dimensionless moment of inertia, see (13) for definition, describes the 'resistance' to rotational versus the 'resistance' to translational body motion due to the mass distribution (see Poulakakis 2002 for more details on the concept of dimensionless moment of inertia). In a diagrammatic

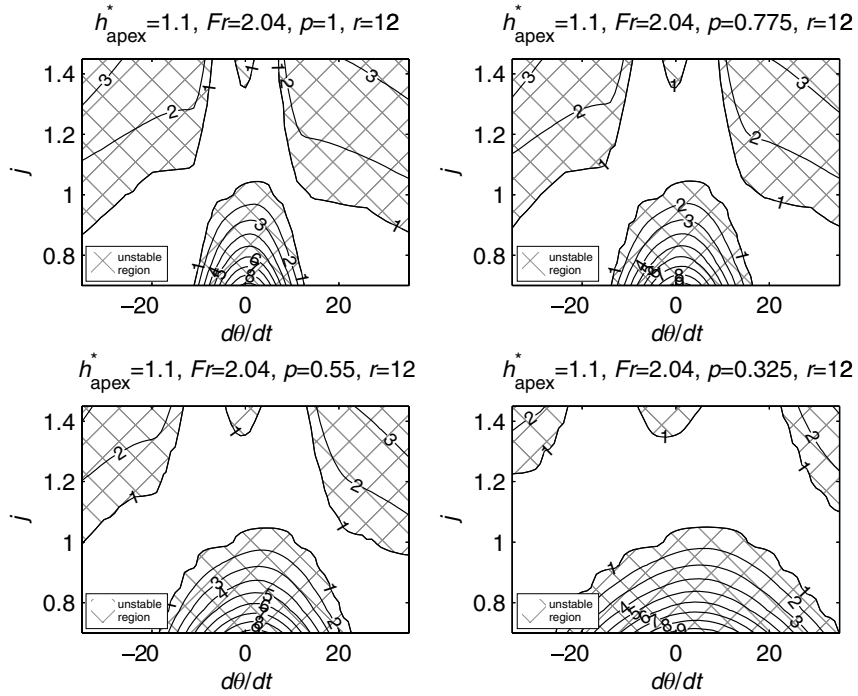

Figure 3. Largest eigenvalue norm at various pitch rates (x axis) and dimensionless body inertias (y axis) for dimensionless apex height 1.1, dimensionless forward speed (Froude number) 2.04, leg relative stiffness 12 and normalised half hip separations from 0.325 to 1.000 (subplots 1–4).

manner, dimensionless body inertia can be thought as two equal point masses that represent the total mass of the system concentrated at the hips of the torso for the case of unit dimensionless body inertia ($J = md^2$), located between the hips for the case dimensionless body inertia greater than one ($J > md^2$) and located outside the hips for the case dimensionless body inertia less than one ($J < md^2$). Note that the distance at which the point masses are located is the radius of gyration, i.e. the distance at which the mass of the system should be concentrated if its moment of inertia is to remain unchanged. Therefore, depending on the location of the equivalent point masses, i.e. the magnitude of the dimensionless moment of inertia, pronking-like motion, where pitch motion is negligible, or bounding, where the pitch motion is dominant, is favoured.

Finding 2. The self-stabilised behaviour of a quadruped robot for a particular gait is related to the magnitude of its body dimensionless inertia. Dimensionless body inertia less than one provides self-stabilising characteristics for bounding motions (high pitch rates), while pronking-like motions (low pitch rates) are self-stable for quadruped robots with dimensionless body inertia greater than one.

3.3. Normalised hip separation

The effect of normalised half hip separation is depicted in Figure 3, as four subplots have been plotted for normalised half hip separation from 0.325 to 1.000. As shown in Figure 2, isolines of the largest eigenvalue norm at various pitch rates and dimensionless body inertias are displayed in Figure 3. The contour plots are drawn for dimensionless apex height 1.1, dimensionless forward speed (Froude number) 2.04 and leg relative stiffness 12, which are again adopted from the Scout II robot (Poulakakis et al. 2006).

The main conclusion drawn by analyzing Figure 3 is that the self-stabilised regime of the quadruped robot is enlarging, while the normalised half hip separation is decreasing. Decreased normalised half hip separation simply means that body length is smaller for the same leg length. Small body length results in increased 'resistance' to rotational motion compared to translational motion, i.e. the hip will move upwards due to linear acceleration instead of moving downwards due to rotational acceleration (see Poulakakis 2002 for more details on the concept of dimensionless moment of inertia). In this case, pitch motion is not favoured and pronking-like motions dominate. For the Scout II robot, for which the 'resistance' against rotational motion is smaller than the 'resistance' against translational motion (dimensionless body inertia less than one, i.e. $J < md^2$), dimensionless hip separation should be as large as possible to allow for self-stable bounding at lower (practically achievable) pitch rates, which is easy to achieve with proper hip placement.

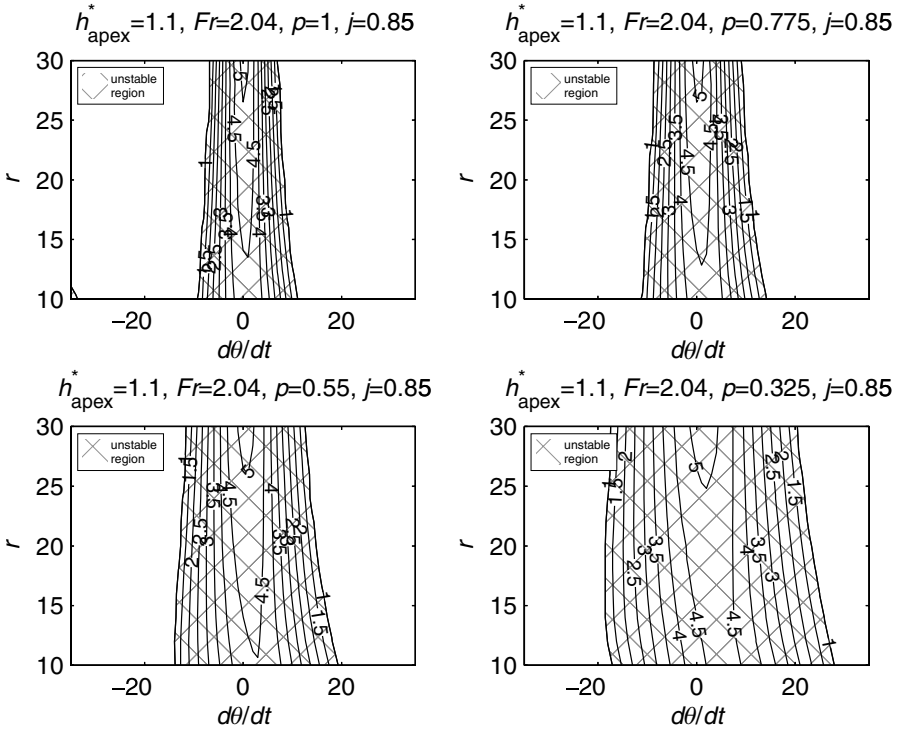

Figure 4. Largest eigenvalue norm at various pitch rates (x axis) and leg relative stiffnesses (y axis) for dimensionless apex height 1.1, dimensionless forward speed (Froude number) 2.04, dimensionless body inertia 0.85 and normalised half hip separations from 0.325 to 1.000 (subplots 1–4).

One may reach to the same conclusion by analysing Figures 4 and 5, where the contour plots of the largest eigenvalue norm at various pitch rates and values of leg relative stiffness are drawn. Once again, the magnitude of the variables has been chosen such as to correspond to the physical parameters of Scout II (Poulakakis et al. 2006).

Specifically, the dimensionless apex height is 1.1 and the dimensionless forward speed (Froude number) is 2.04. In Figure 4, the dimensionless body inertia is 0.850, as in Scout II, while in Figure 5 the dimensionless body inertia is chosen to be 1.225 to demonstrate the effect of relative leg stiffness on quadruped robots with dimensionless body inertia greater than one. The effect of normalised half hip separation is represented graphically by Figures 4 and 5, as the four subplots in each figure have been plotted for normalised half hip separation from 0.325 to 1.000.

In Figure 4, it is evident that the self-stabilised regime of bounding quadruped robots with dimensionless body inertia less than one is enlarging, while the normalised half hip separation is increasing. Contrastingly, as Figure 5 implies, normalised half hip separation should be decreased for quadruped robots with dimensionless body inertia greater than one that pronk or bound at low pitch rates so as to enlarge their self-stabilised regime. A specific value of normalised half hip separation is easy to attain by proper hip placement.

Finding 3. The self-stabilised regime of pronking-like motions (low pitch rates) for quadruped robots with dimensionless body inertia greater than one is enlarging, while the normalised half hip separation is decreasing. Larger dimensionless hip separation allows for self-stable bounding at a wider range of pitch rates for quadruped robots with dimensionless body inertia less than one.

3.4. Relative leg stiffness

With respect to the effect of leg relative stiffness on the stability of the motion and the self-stabilising characteristics of the robot, two conclusions are drawn by analysing Figures 4 and 5. On the basis of Figure 4, the self-stabilised regime of bounding quadruped robots with dimensionless body inertia less than one is enlarging, while the relative leg stiffness is increasing. Contrastingly, based on Figure 5, relative leg stiffness should be decreased for quadruped robots with dimensionless body inertia greater than one that pronk or bound at low pitch rates so as to enlarge their self-stabilised regime.

The former can be explained by the fact that harder springs at legs, a typical case where leg relative stiffness is increased, result in less compression along the leg during leg–ground interaction, which typically leads to less pitching. Since the ‘resistance’ against rotational motion

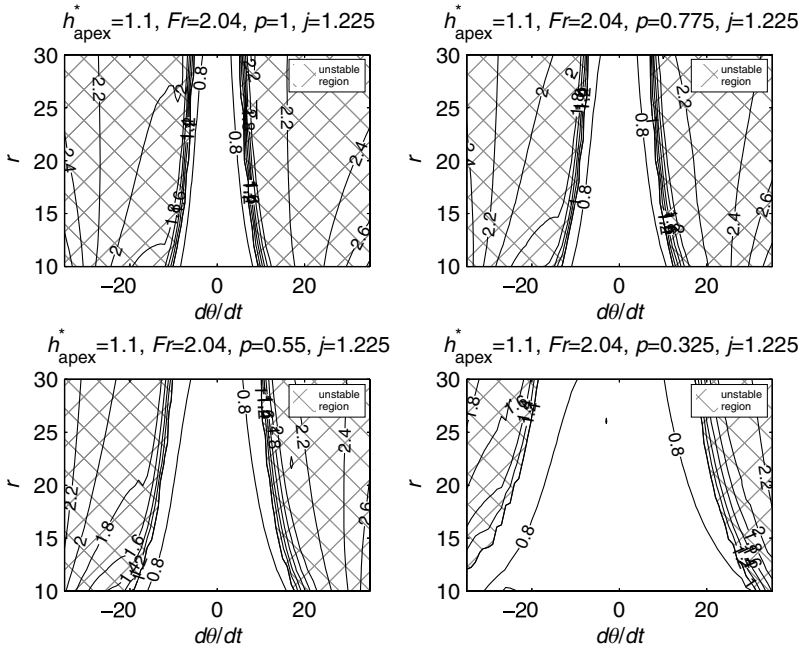

Figure 5. Largest eigenvalue norm at various pitch rates (x axis) and leg relative stiffnesses (y axis) for dimensionless apex height 1.1, dimensionless forward speed (Froude number) 2.04, dimensionless body inertia 1.225 and normalised half hip separation from 0.325 to 1.000 (subplots 1–4).

is smaller than the 'resistance' against translational motion when $J < md^2$ (dimensionless body inertia less than one), self-stable motions at lower pitch rate are possible (see Figure 4 to graphically visualise this).

On the other hand, leg relative stiffness is increased when the mass of the system is decreased in a proportional manner (see (14) for definition). Smaller mass means that the 'resistance' against translational motion is less or equivalently that the 'resistance' against rotational motion is dominant. In that case, i.e. for quadruped robots with dimensionless body inertia less than one ($J > md^2$), lower pitch rates are required to allow for self-stabilising behaviour (see Figure 5 for depiction).

Finding 4. Leg relative stiffness for a quadruped robot should be chosen according to the magnitude of the dimensionless body inertia. Dimensionless body inertia less than one suggests that relative leg stiffness should be as large as possible to enlarge the self-stable regime of the system. Contrastingly, relative leg stiffness should be decreased for quadruped robots with dimensionless body inertia greater than one that pronk (or bound at low pitch rates) so as to enlarge their self-stabilised regime.

4. Guidelines

Taking into account the above-mentioned findings, the following design guidelines could be proposed for Scout II quadruped robot that might improve its performance:

(1) Scout II would passively bound at lower forward speeds by changing the value of its dimensionless body inertia. By attaining a value of dimensionless body inertia that is greater than one, it would obtain self-stabilising characteristics even for pronking-like motions. This is easily attained by proper hip placement or body mass redistribution.
(2) Scout II would be able to perform self-stable bounding behaviour at lower and practically achievable pitch rates, even if its dimensionless body inertia is kept less than one, by increasing its normalised hip separation. This could be easily achieved either by proper hip placement or by shortening its legs rest length.
(3) The self-stabilised regime of the existing Scout II bounding robot could be further enlarged if its legs relative stiffness is increased, which could be attained simply by increasing its legs' spring stiffness or by shortening their rest length.

5. Conclusion

The stability analysis of the passive dynamics of robotic quadrupeds was studied in a dimensionless context, revealing further intrinsic properties of quadrupedal running and unveiling aspects of robotic quadrupeds that have similar configuration but different scale. It was shown that suitable mechanical design of the quadruped robot can provide self-stabilising characteristics against external perturbations

originated in leg–ground interactions and motor control and result in dynamically stable running with bounding and pronking gaits with physically realistic and practically achievable forward speeds and pitch rates. We anticipate that the proposed guidelines will assist in the design of new, and modifications of existing, quadruped robots. These can be summarised in (a) greater forward speeds enlarge the self-stable regime of quadruped running robots, (b) the self-stabilised behaviour of a quadruped robot for a particular gait is greatly related to the magnitude of its dimensionless body inertia and (c) the values of dimensionless hip separation and leg relative stiffness of a quadruped running robot affect the stability of its motion and should be in inverse proportion to its dimensionless body inertia. It is simple for a quadruped robot to attain a specific value of dimensionless body inertia by redistributing its body mass, a specific value of dimensionless hip separation by proper hip placement and a specific value of relative leg stiffness by adjusting leg spring stiffness.

Acknowledgements

Support by public (European Social Fund 80% and General Secretariat for Research and Technology 20%) and private funds (Zenon SA), within measure 8.3 of Op. Pr. Comp., 3rd CSP-PENED 2003, is acknowledged.

References

Ahmadi M, Buehler M. 1997. Stable control of a simulated one-legged running robot with hip and leg compliance. IEEE Trans Robo Autom. 13(1):96–104.

Alexander RMcN. 1977. Terrestrial locomotion. Mechanics and energetics of animal 1ocomotion. London: Chapman & Hall.

Berns K. 2008. Walking machine catalogue. Available from: http://www.walking-machines.org/.

Blickhan R. 1989. The spring-mass model for running and hopping. J Biomech. 22:1217–1227.

Buehler M. 2002. Dynamic locomotion with one-, four- and six-legged robots. J Robot Soc Jpn. 20(3):15–20.

Chatzakos P, Papadopoulos E. 2009. Bio-inspired design of electrically-driven bounding quadrupeds via parametric analysis. Mech Mach Theory. 44(3):559–579.

Cherouvim N, Papadopoulos E. 2005. Single actuator control analysis of a planar 3DOF hopping robot. Robotics: science and systems I. Cambridge (MA): MIT Press. p. 145–152.

Farley CT, Glasheen J, McMahon TA. 1993. Running springs: speed and animal size. J Exp Biol. 185:71–86.

Full RJ, Koditschek D. 1999. Templates and anchors: neuromechanical hypotheses of legged locomotion on land. J Exp Biol. 202:3325–3332.

Ghigliazza RM, Altendorfer R, Holmes P, Koditschek DE. 2003. A simply stabilized running model. SIAM J Appl Dyn Syst. 2(2):187–218.

Herr HM, Huang GT, McMahon TA. 2002. A model of scale effects in mammalian quadrupedal running. J Exp Biol. 205(7):959–967.

Iida F, Pfeifer R. 2004. Cheap rapid locomotion of a quadruped robot: self-stabilization of bounding gait. Intelligent Autonomous Systems 8. Amsterdam, The Netherlands: IOS Press. p. 642–649.

Kimura H, Fukuoka Y, Cohen AH. 2007. Adaptive dynamic walking of a quadruped robot on natural ground based on biological concepts. Int J Robot Res. 26(5):475–490.

Kubow T, Full R. 1999. The role of the mechanical system in control: a hypothesis of self-stabilization in hexapedal runners. Philos Trans R Soc Lond Ser B – Biol Sci. 354(1385):854–862.

McMahon T. 1985. Muscles, reflexes, and locomotion. Princeton University Press, NJ, USA.

Murphy KN, Raibert MH. 1984. Trotting and bounding in a planar two-legged model. In: Morecki A, Bianchi G, Kedzior K, editors. 5th symposium on theory and practice of robots and manipulators. Cambridge (MA): MIT Press. p. 411–420.

Papadopoulos E, Cherouvim N. 2004. On increasing energy autonomy for a one-legged hopping robot. IEEE international conference on robotics and automation; New Orleans, LA, USA. p. 4645–4650.

Pearson K. 1976. The control of walking. Sci Am. 72:86.

Poulakakis I. 2002. On the passive dynamics of quadrupedal running [master of engineering thesis]. Montreal, QC, Canada: McGill University.

Poulakakis I, Papadopoulos EG, Buehler M. 2006. On the stability of the passive dynamics of quadrupedal running with a bounding gait. Int J Robot Res. 25(7):669–687.

Raibert MH. 1986. Legged robots that balance. Cambridge (MA): MIT Press.

Reynolds O. 1883. An experimental investigation of the circumstances which determine whether the motion of water shall be direct or sinuous, and of the law of resistance in parallel channels. Philos Trans R Soc. 17:935–982.

Saranli U, Koditschek DE. 2003. Template based control of hexapedal running. IEEE Int Conf Robo Autom. 1:1374–1379.

Schwind W. 1998. Spring loaded inverted pendulum running: a plant model [PhD thesis]. [Ann Arbor (MI)]: University of Michigan.

Seyfarth A, Geyer H, Guenther M, Blickhan R. 2002. A movement criterion for running. J Biomech. 35:649–655.

Zhang ZG, Fukuoka Y, Kimura H. 2004. Stable quadrupedal running based on a spring-loaded two-segment legged model. IEEE Int Conf Robot Autom. 3:2601–2606.